Journal of Visualization, Vol. 5, No. 2 (2002) 177-186

Visualization of the Tidal Flow in Sasebo and Oomura Bays

Kikukawa, H.*1, Segawa, M.*1 and Kohno, J.*2

*1 Department of Environmental and Information Sciences, Faculty of Fisheries, Kagoshima University, Shimoarata 4-50-20, Kagoshima 890-0056, Japan.
*2 Kagoshima Environmental Research and Service, Nanatsushima 1-1-5, Kagoshima 891-0132, Japan.

Received 22 October 2001.
Revised 21 January 2002.

***Abstract*:** Sasebo and Oomura Bays situated in the northwest of Kyushu, Japan form a coupled bay linked by a channel. The tidal flow in and between these bays is visualized by the satellite images and the dispersion of Lagrangian particles is numerically studied. The satellite images are available to visualize the tidal flow at the mouth of Hario-seto from the maximum flood tide to the end of ebb tide at Tainoura. The seawater plume from the mouth of Hario-seto goes southeastward and then rotates anti-clockwise. The time of one rotation is about 6 to 7 periods. The plume extends about 10 km from the mouth of Hario-seto. Lagrangian particles in Sasebo Bay also flow into Oomura Bay through Haiki-seto.

***Keywords*:** coupled bay, satellite image, Lagrangian particle, dispersion, plume, tidal flow.

1. Introduction

Oomura Bay is connected to Sasebo Bay through Hario-seto and Haiki-seto (Fig. 1). As Haiki-seto is very narrow and long, most of water exchanges through Hario-seto, whose width is about 200 m with 25 m depth. Sasebo Bay is opened to East China Sea, whose mouth is about 800 m in width. These two bays make a unique coupled bay.

Oomura Bay is not only useful for the marine products but also related to the tourist trades and the surrounding industries. In recent years, the environment of the seawater is becoming worse due to the industrial activities along the coast. Thus to preserve the seawater in good condition is an earnest problem.

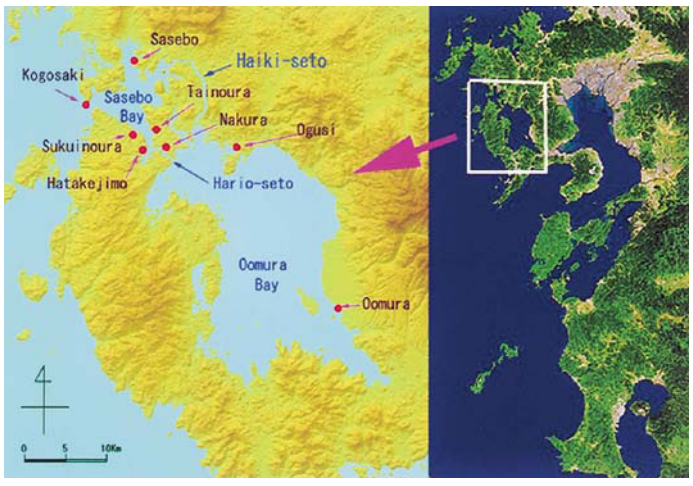

Fig. 1. Map of Sasebo and Oomura Bays.

Part of the seawater purgation is played by the tidal water mass exchange. The tidal current disperses the contaminated matters and prevents from the extreme pollution. As the depth of Oomura Bay is less than 20 m for the most part, the density current in winter could not be effective for the purgation.

The observation of the water mass exchange at a mouth of a bay (Sakurai, 1983) cannot clearly distinguish the tidal water exchange from the ones caused by the wind driven and the density flows. Numerical simulation is suited to estimate the tidal flow. The seawater exchange in a bay is studied numerically by estimating the tidal residual flow (Kikukawa and Ichikawa, 1990) and by the dispersion of Lagrangian particles (Segawa et al., 1998; Kohno et al., 2001). The tidal current could not generally be seen in the satellite images, although the tidelands come out in e.g. Ariake Sea at low water and a cold water mass tends to appear around the mouth of a bay at the maximum ebb current.

In this article, we try to visualize the tidal water mass exchange in Oomura Bay, for the purpose of knowing the role of the tidal current for the seawater purification. The visualization by the satellite images is given first, since it is exceptionally valid in Oomura Bay, and then the dispersion of the imaginary Lagrangian particles is numerically studied.

2. Visualization by Satellite Images

In most cases, the visualization of the seawater flow by the satellite images is performed using the altimeter data (Ichikawa and Imawaki, 1994; Aoki et al., 1995) or employing the sea surface temperature (Kouzai and Tsuchiya, 1990; Kubota and Shirota, 1993; Tsutsumi et al., 1999). When the sea is muddy due to red tide, pollution, river flood etc., the visible and near infra-red remote sensings are also available (Hyodo et al., 1997). In the case of Oomura Bay, the sea surface temperature visualization is effective in winter and the visible and near infra-red one in summer.

Figure 2 shows the examples of the visualization of the tidal flow around the mouth of Hario-seto by Landsat5/TM image on Sep. 17, 1992. The single band and the false color visualizations depend on which bands we select. In the maximum likelihood method, several training data have to be selected first, then the data of each pixel in the satellite image are identified to some training data having maximum likelihood. Thus the maximum

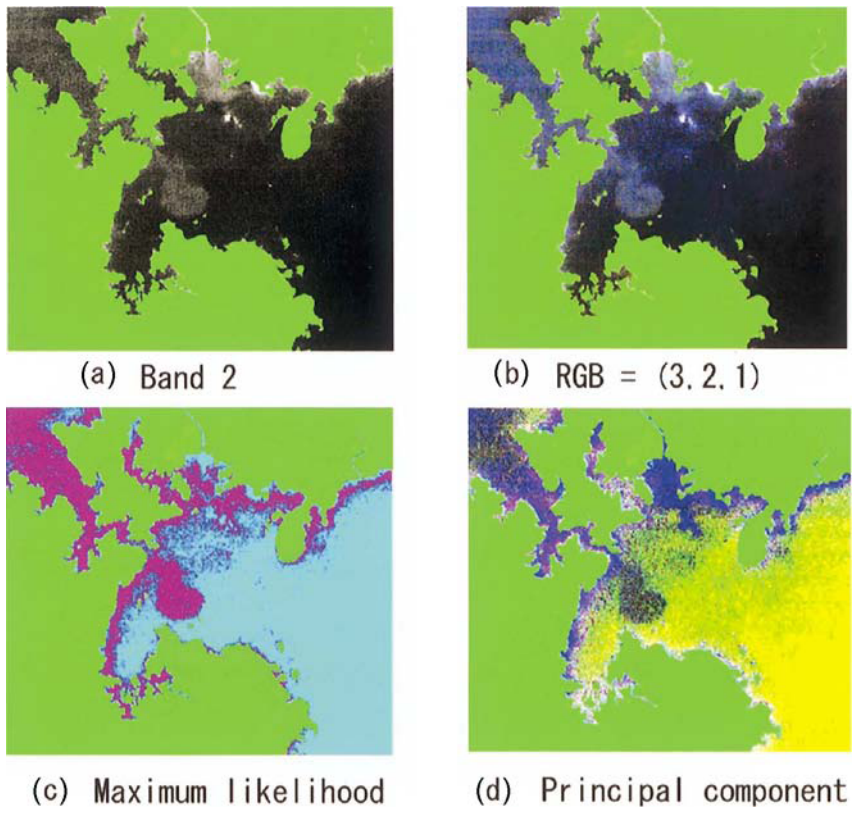

Fig. 2. Examples of the visualization methods of the tidal flow using the satellite image of Sep. 17, 1992. (a) single band, (b) false color, (c) maximum likelihood method, (d) principal component method.

likelihood visualization depends on the selected training data and the tidal fine structures are invisible, although it utilizes all bands and then becomes available in one year. In the principal component method, the principal components of the image data are estimated in the object area and then used as the false color visualization. Then the principal component visualization makes use of all bands and the detailed tidal structure is preserved. Thus we employ the principal component visualization.

In Fig. 3, the tidal flow around the mouth of Hario-seto is shown using the principal component visualization. The sea levels at Tainoura (blue line) and at Ogusi (pink line) are calculated using the tidal harmonic coefficients of the sea level (The Maritime Safety Agency, 1973) and are shown in the figures with the time of satellite observation (vertical green line). The figures are put in the order of the sea levels. The tidal harmonic coefficients of current are not available there, but the phase of the tidal current generally advances about 90 degrees from the one of the sea level. Thus, we can speculate the phase of the tidal current from the sea level. In Fig. 3, the

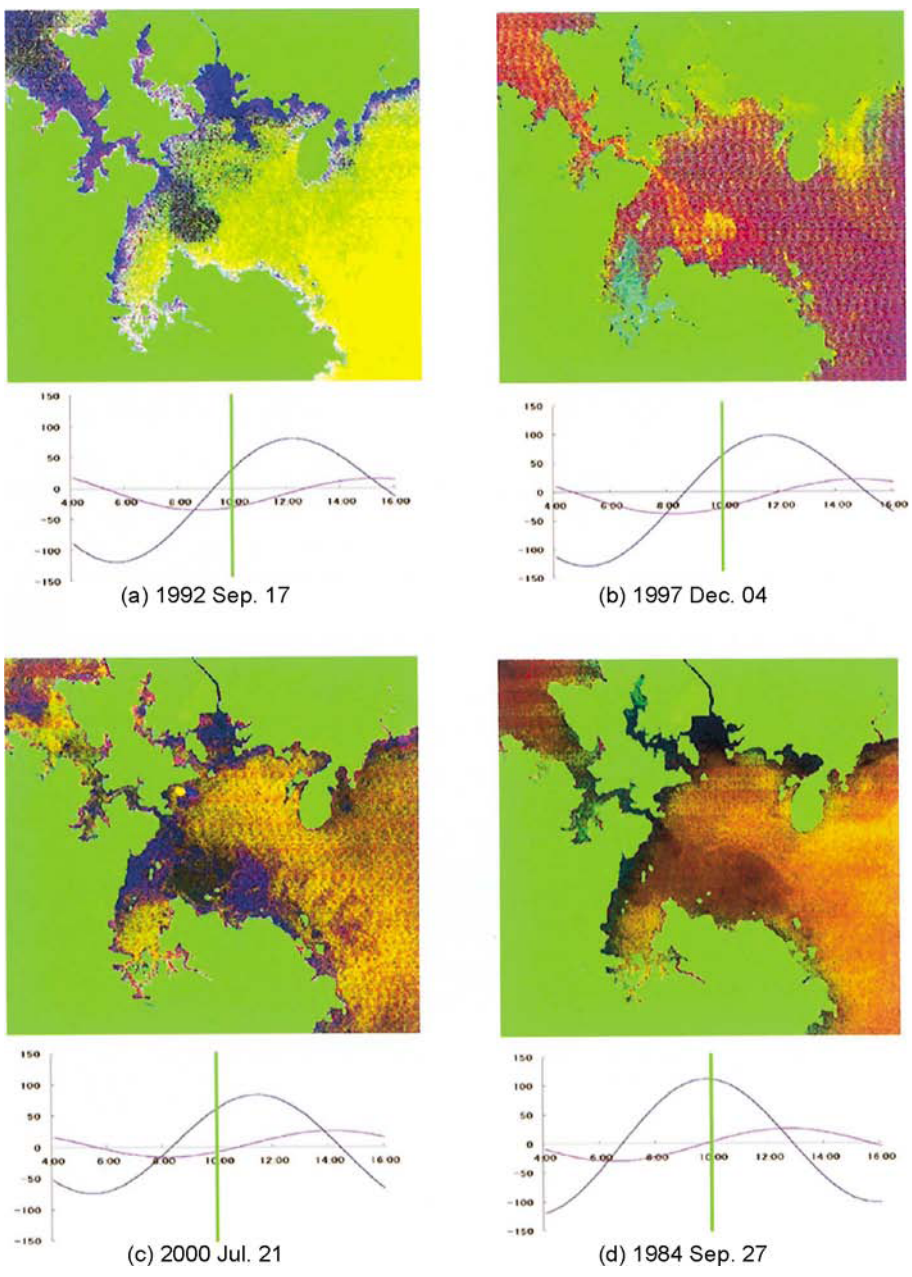

Fig. 3. Visualizations of the tidal flow using the principal component method of the satellite images with the sea levels at Tainoura (blue line) and at Ogusi (pink line). Vertical green lines denote the time of the satellite observation. Pictures are put in the order of the sea level. (continued to page 180)

incoming seawater from Hario-seto and that of Oomura Bay can be distinguished from the time of the maximum flood tide to the end of ebb tide at Tainoura. From the time of the beginning to the maximum flood tide at Tainoura, the distinction of the seawater is unclear. In that period, the seawater in Oomura Bay and in Sasebo Bay might be mixed each other and the temperature and color resembled. We could not see the assimulation of the seawater from the dispersion of Lagrangian particles. For that purpose, the simulation of the temperature and color is indespensable and more physical parameters have to be decided.

The incoming seawater from the mouth of Hario-seto first looks as a jet (Figs. 3(a) to 3(b)), extends southeastward for about 10 km from the exit (Figs. 3(c) to 3(d)), and then rotates anti-clockwise (Figs. 3(e) to 3(f)). After the time of the maximum ebb tide at Tainoura, the seawater in Oomura Bay seems to outflow through Hario-seto (Figs. 3(g) to 3(h)). The results shown in Fig. 3 are essentially the same as those given by Hyodo et al. (1997) using the maximum likelihood visualization.

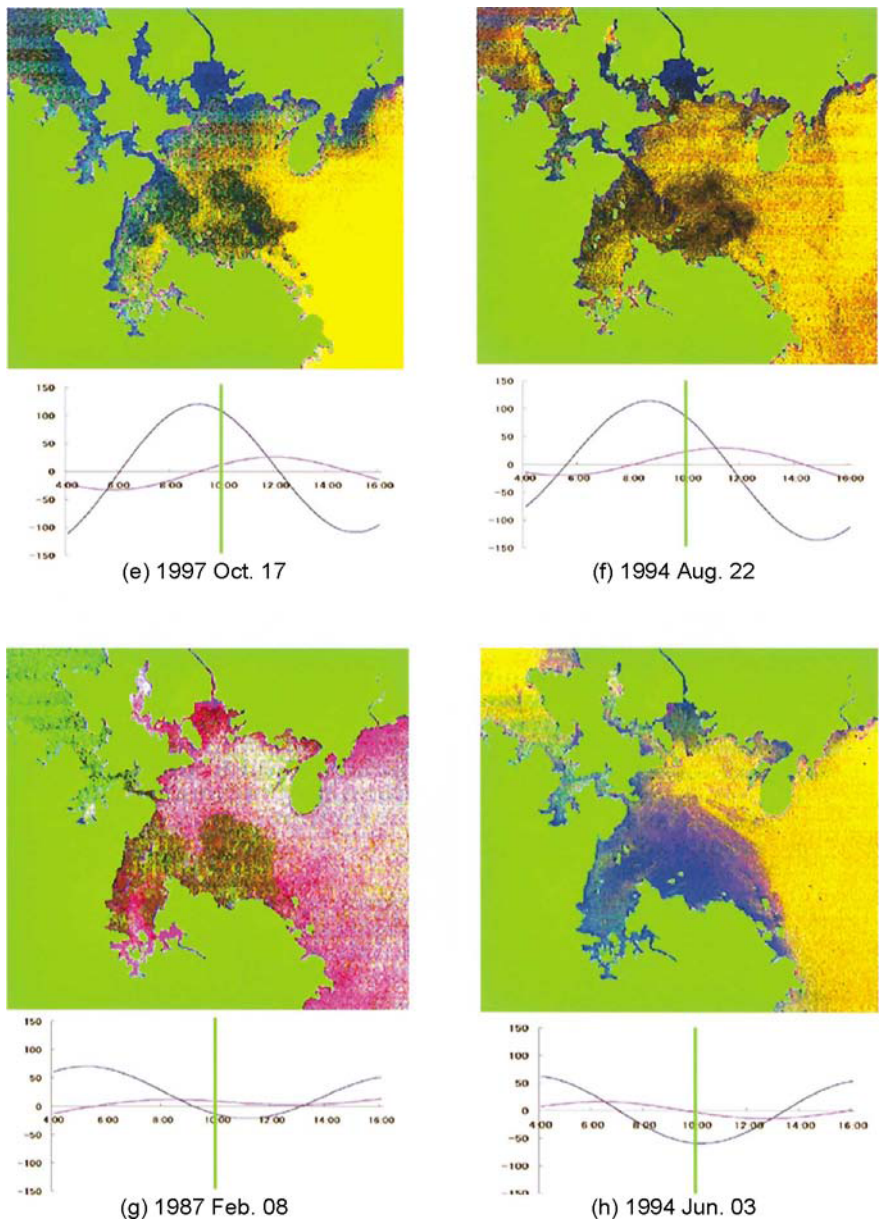

(e) 1997 Oct. 17 (f) 1994 Aug. 22

(g) 1987 Feb. 08 (h) 1994 Jun. 03

Fig. 3. (continued from page 179)

3. Visualization by Lagrangian Particles

This section is devoted to the visualization of the tidal flow by Lagrangian particles, the behavior of which is numerically simulated. In the finite element method (FEM), the object area is divided by the triangular elements, in contrast to the rectangular ones in the finite difference method (FDM), and is suited to trace the complex coastline. It is also easy in FEM to study the interesting region deeper using smaller elements. Thus we adopt FEM to simulate the tidal flow, since the topography of Hario-seto is complex.

The numerical simulation is performed improving the control volume based two-dimensional FEM (Baliga and Patankar,1983) to be available for the equation of evolution. Because the method of simulation is the same as the one written in Kohno et al. (2001), only the triangular division of the area (Fig. 4) and the depth distribution (Fig. 5) are presented. The numbers of nodes and elements are 8806 and 15038, respectively. The depth at every node is read from Fig. 5. At the open boundary in Fig. 4, the sea level η is forced to be

$$\eta = a \sin(\omega_M t - \delta), \quad \omega_M = 2\pi/45000\ (s^{-1}), \quad a = 82.0\ (cm), \quad \delta = 240.0\ (degree),$$

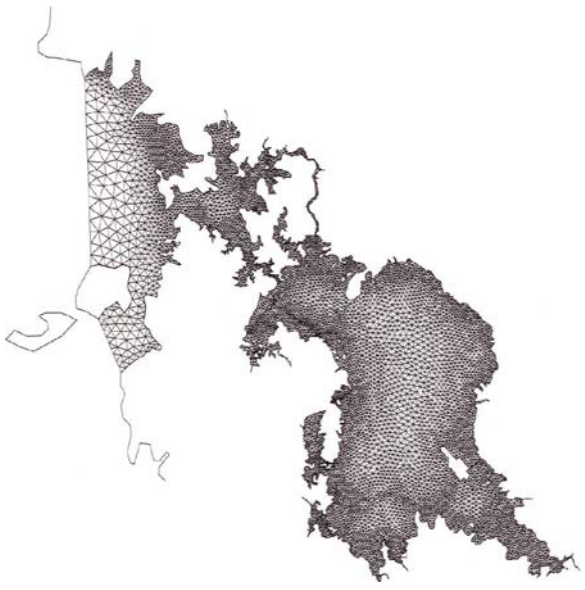

Fig. 4. Division of Sasebo and Oomura Bays by the triangular elements.

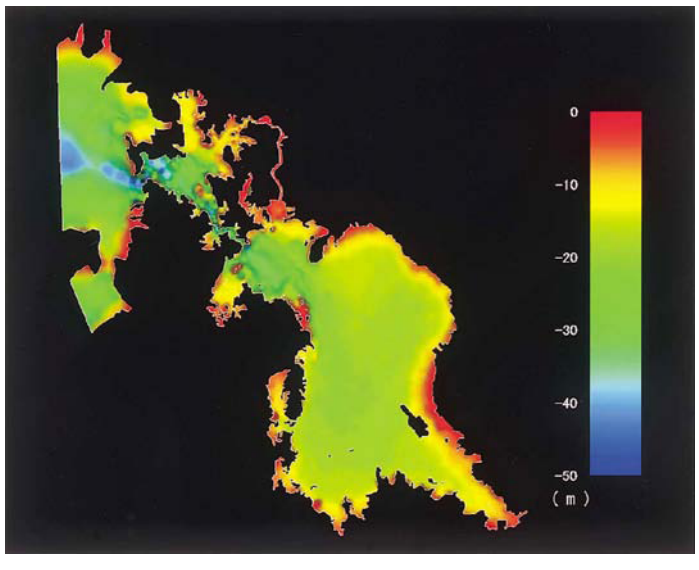

Fig. 5. Depth distribution used in our simulation.

which is the M_2 harmonic sea level at Kogosaki. The slip boundary condition is adopted at the coast, because with the horizontal eddy viscosity and the bottom friction, the phase of the sea level is calculated appropriately. Initially, the still seawater and the flat sea surface are assumed. The calculated velocity and the sea level became stable after 10 periods.

The calculated sea levels at several points are compared with the tidal harmonic constants of the semi-diurnal tide in Fig. 6. Abscissa denotes the sea level observation stations shown in Fig. 1. We can see that the calculated amplitudes and phases are almost equal to the harmonic ones in spite of giving only the M_2 tidal sea level at the open boundary. When the tidal wave progresses through Hario-seto, the amplitude decreases by about 60 cm and the phase delays by about 80 degrees. The calculated amplitude at Hatakejimo, which lies in the small inlet in Hario-seto, is a little smaller than the observed one. This fact implies the necessity of the smaller triangular division for such a small inlet, or to devise the coastal boundary condition.

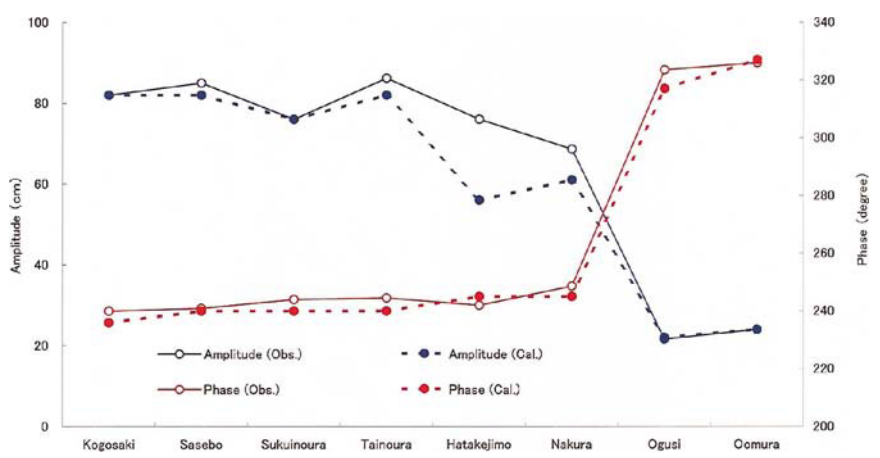

Fig. 6. Comparison of M_2 tidal coefficients between the observation and the calculation. Abscissa denotes the sea level observation stations shown in Fig. 1.

In Fig. 7 the dispersion of Lagrangian particles in Sasebo Bay is shown. After the preliminary 10 periods calculation, Lagrangian particles are put into the bay and the particle dispersion is calculated during 50 periods. The jet is seen at the mouth of Hario-seto. At the 6th period, the incoming particles begin to form a cluster, which seems to stay at almost the same location afterward. The position of the cluster looks like a little closer to the mouth of Hario-seto than those shown by the satellite images in Fig. 3. As written in Kohno et al. (2001), we have adopted the bottom friction parameter c_f = 0.0026/depth and Smagorinsky's model (Miyata, 1995) for horizontal eddy viscosity; $\upsilon_e = (C_s \Delta)^2 \sqrt{2\overline{S_{ij}}\overline{S_{ij}}}$, where S_{ij} is the rate-of-strain tensors, overline space averaging, Δ the space filter width, with C_s = 0.25. The changes of these parameters could affect the position of the cluster. Another cause of disagreement might be the effect of wind, which is not estimated in our calculation. The wind direction at 10 a.m., when the satellite images are taken, tends to be eastward, i.e. the wind from East China Sea. Thus the wind could extend the diffusion area. However, we are satisfied with the reproduction of the jet-like inflow and the cluster remaining almost the same location, which is realized in the satellite images in Fig. 3.

Another aspect in Fig. 7 is the flow through Haiki-seto, which is very narrow and long. The Lagrangian particles passed through Haiki-seto after 15th period and flowed into Oomura Bay. After the inflow, the particles make a line and march along the coast to the mouth of Hario-seto. The flow from the mouth of Haiki-seto to that of Hario-seto is not clearly seen by the satellite images in Fig. 3, although the water mass at the mouth of Haiki-seto tends to be similar to the one in Sasebo Bay. We cannot explain satisfactorily why Lagrangian particles pass through Haiki-seto into Oomura Bay. Only we denote the fact that the average sea level at Sasebo is 102 cm higher than the one at Oomura.

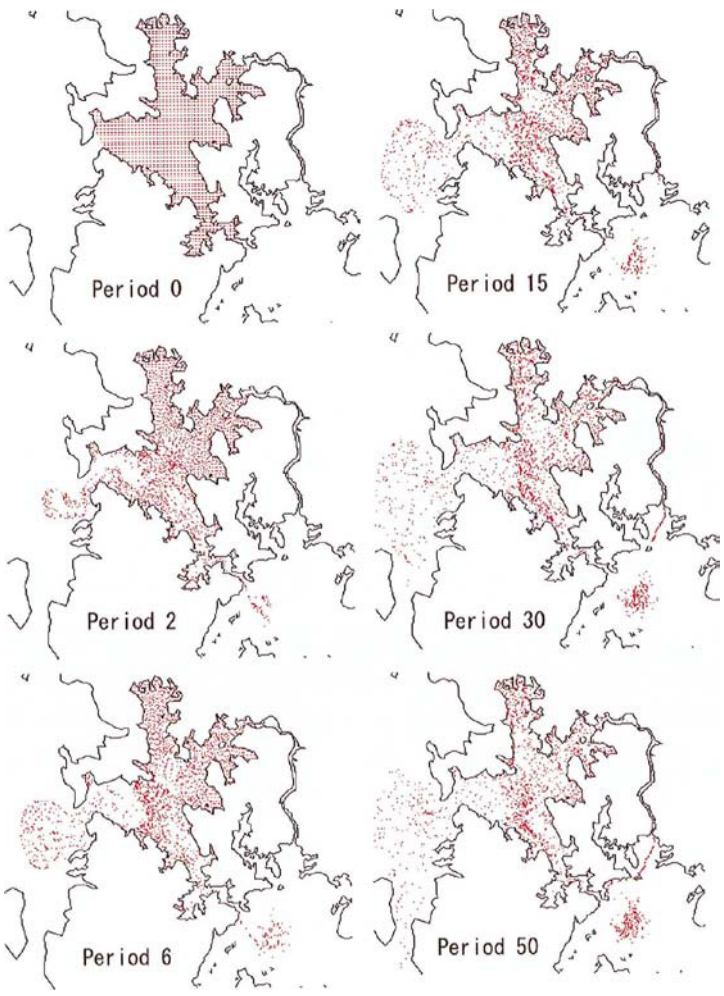

Fig. 7. Dispersion of Lagrangian particles initially put in Sasebo Bay.

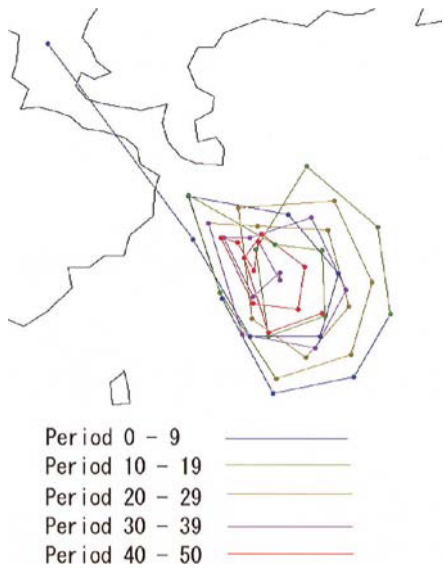

Fig. 8. Locations of a Lagrangian particle initially placed at Hario-seto, at the end of each period.

Figure 8 shows the trajectory of one Lagrangian particle during 50 periods initially placed in Hario-seto. The trajectory is drawn by linking the location at the same phase of each period. The existence of anti-clockwise vortex around the mouth of Hario-seto is clearly indicated. The time to make one rotation is generally 6 to 7 periods, and the diameter decreases with period. The rotation might be attributed to the topography of the bay and the induced tidal residual flow, althrough the behavior of a Lagrangian particle cannot be fully understood by the residual flow.

Actually, a Lagrangian particle moves with the instantaneous tidal flow. The Lagrangian particles initially located in Hario-seto (red particles) and at the mouth of Hario-seto (blue particles) move with the ebb and flood tidal flow as shown in Fig. 9. The anti-clockwise movement at the mouth of Hario-seto is also seen in the figure.

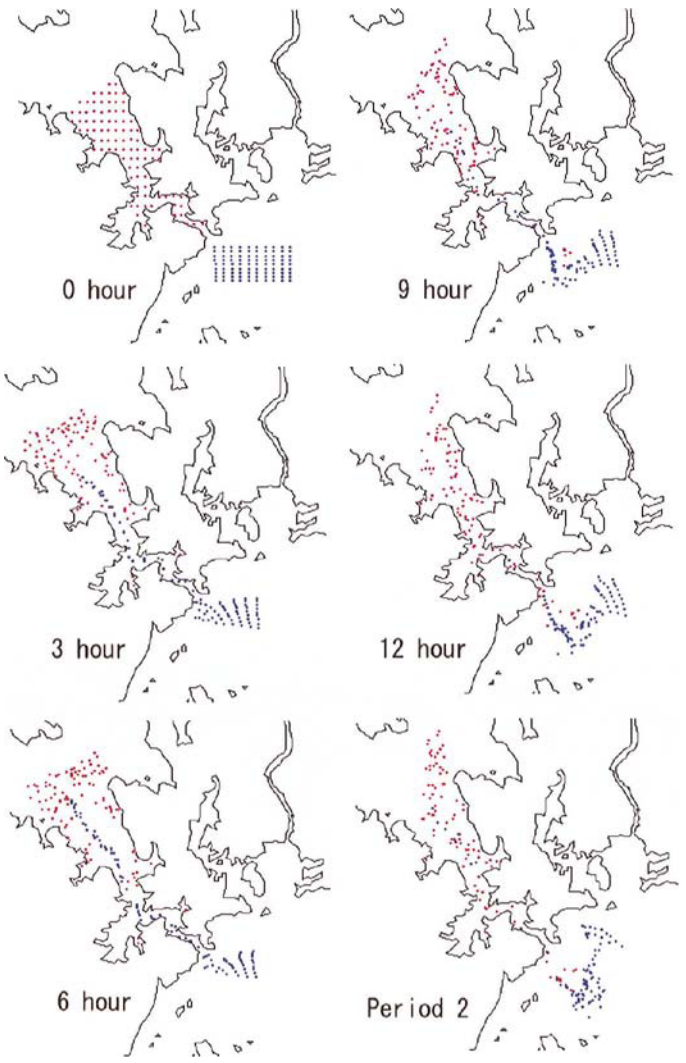

Fig. 9. Locations of Lagrangian particles initially placed around Hario-seto at 3, 6, 9 and 12 hour in Period 1 and at the end of Period 2.

The traces of 4 representative Lagrangian particles are shown in Fig. 10. A trace is drawn by linking the location of a Lagrangian particle at each 10 minutes during 50 periods. The Lagrangian particles do not go so far from their initial location, except the one passing through Haiki-seto.

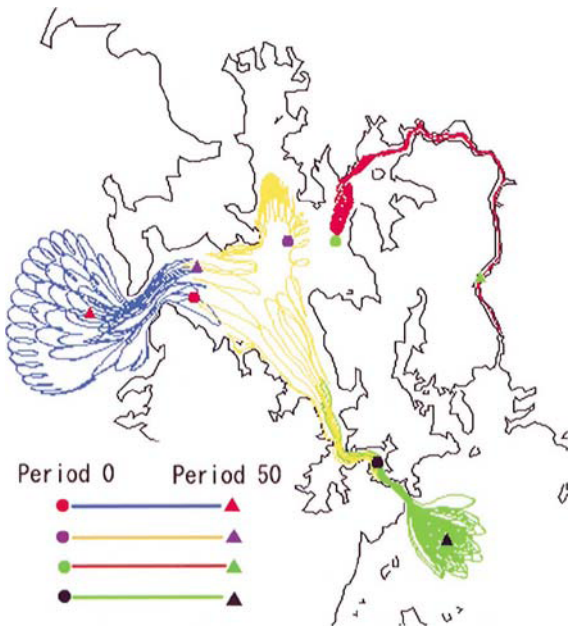

Fig. 10. Examples of 4 particle traces during 50 periods, initially placed in Sasebo Bay and Hario-seto.

4. Conclusion

Sasebo and Oomura Bays are situated in northwest of Kyushu, Japan, and form a coupled bay connected by a channel. The sea water exchanges through Hario-seto, whose width is about 200 m. Visualization of the tidal flow around the mouth of Hario-seto is performed by the satellite images and the dispersion images of Lagrangian particles. The principal component visualization by the satellite images is found to be available from the maximum flood tide to the end of ebb tide at Tainoura. The seawater coming into Oomura Bay through Hario-seto makes a plume, and extends for about 10 km from the mouth of Hario-seto. The plume then rotates anti-clockwise. The dispersion images of Lagrangian particles show that the time of making one rotation is about 6 to 7 periods. Lagrangian particles in Sasebo Bay are also found to flow into Oomura Bay through Haiki-seto.

References

Aoki, S., Imawaki, S. and Ichikawa, K., Baroclinic Disturbances Propagating Westward in the Kuroshio Extension Region as Seen by a Satellite Altimeter and Radiometers, Journal of Geophysical Research, 100 (1995), 839-855.

Baliga, B. R. and Patankar, S. V., A Control Volume Finite-Element Method for Two-dimensional Fluid Flow and Heat Transfer, Numerical Heat Tranfer, 6 (1983), 245-261.

Hyodo, R., Gotoh, K. and Jun, B., Investigation of Ocean Current in Closed Bay Using Remote Sensing Technique and its Availability, Environmental Engineering Research, 34 (1997), 143-154 (in Japanese).

Ichikawa, K. and Imawaki, S., Life History of a Cyclonic Ring Detached from the Kuroshio Extension as Seen by the Geosat Altimeter, Journal of Geophysical Research, 99 (1994), 15953-15966.

Kikukawa, H. and Ichikawa, H., A Numerical Study of a Tide with Four Harmonic Constituents at the Open Boundary, Journal of the Oceanographical Society of Japan, 46 (1990), 143-155.

Kohno, J., Kikukawa, H. and Ueda, K., Numerical Study of Tidal Water Mass Exchange in an Inland Sea with Archipelago, Journal of Visualization, 3-4 (2001), 369-378.

Kouzai, K. and Tsuchiya, K., Estimation of Surface Current Velocities of the Kuroshio Using Single NOAA/AVHRR Image, Journal of the Remote Sensing Society of Japan, 10 (1990), 325-335.

Kubota, M. and Shirota, M., Method for Estimating Sea Surface Velocity from NOAA/AVHRR Images, Umino Kenkyu, 2 (1993), 169-187 (in Japanese).

The Maritime Safety Agency, The Table of Tidal Harmonic Coefficients, (1973) (in Japanese).

Tsutsumi, K., Kohno, J., Anraku, K., Kikukawa, H., Shimozono, K. and Kinoshita, K., Study of River Water Expansion in the Inner Kagoshima Bay by the Infrared Remote Sensing, Journal of the Remote Sensing Society of Japan, 19 (1999), 37-49 (in Japanese).

Miyata, H., Analysis of Turbulent Flows, (1995), The University of Tokyo Press, Tokyo, 79-84 (in Japanese).

Sakurai, M., Water Exchange through the Mouth of Kagoshima Bay, Bulletin on Coastal Oceanography, 21 (1983), 45-52 (in Japanese).

Segawa, M., Kohno, J. and Kikukawa, H., Numerical Study of Tidal Water Mass Exchange in Ikara-seto, Memoirs of Faculty of Fisheries Kagoshima University, 47 (1998), 25-33 (in Japanese).

Author Profile

Hiroyuki Kikukawa: He is a professor of environmental and information sciences in the faculty of fisheries at Kagoshima University. He received his B.Sc. (1967) and his Ph.D. (1973) in Physics from The University of Tokyo. After Ph.D., he works at Kagoshima University (1974-) in the field of coastal oceanography. His research interests are satellite remote sensing and numerical study on the coastal environment.

Makoto Segawa: He received his B.F. (1997) and his M.F. (1999) from Kagoshima University. He is a staff of Nagasaki prefectural government. His research interest is the environment of coastal bay.

Jun-ichi Kohno: He received his B.Sc. (1976) and his Ph.D. (1984) in Physics from Kyushu University. From 1993, he serves as a researcher for Kagoshima Environmental Research and Service. His research interests are environmental fluid dynamics and satellite remote sensing.